Journal of Power Sources 182 (2008) 585–588

Contents lists available at ScienceDirect

Journal of Power Sources

journal homepage: www.elsevier.com/locate/jpowsour

Short communication

High-performance cathode-supported SOFCs prepared by a single-step co-firing process

Mingfei Liu [a], Dehua Dong [b], Fei Zhao [a], Jianfeng Gao [a], Dong Ding [a], Xingqin Liu [a], Guangyao Meng [a,*]

[a] Department of Materials Science and Engineering, University of Science and Technology of China, Hefei, 230026 Anhui, China
[b] Department of Chemical Engineering, Monash University, Clayton, Vic. 3800, Australia

ARTICLE INFO

Article history:
Received 16 March 2008
Received in revised form 17 April 2008
Accepted 17 April 2008
Available online 26 April 2008

Keywords:
Cathode-supported
Co-firing
SOFC
$Pr_{0.35}Nd_{0.35}Sr_{0.3}MnO_{3-\delta}$/SDC
YSZ

ABSTRACT

Cathode-supported solid oxide fuel cells (SOFCs), comprising porous $Pr_{0.35}Nd_{0.35}Sr_{0.3}MnO_{3-\delta}$ (PNSM)/$Sm_{0.2}Ce_{0.8}O_{1.95}$ (SDC) cathode supports, SDC function layers, YSZ electrolyte membranes and NiO/SDC anode layers, were successfully fabricated via suspensions coating and single-step co-firing process. The microstructures of electrolyte membranes were observed with scanning electron microscope (SEM). The assembled single cell was electrochemically characterized with humidified hydrogen as fuel and ambient air as oxidant. The open circuit voltage (OCV) of the cell was 1.036 V at 650 °C, and the peak power densities were 657, 472, 290 and 166 mW cm^{-2} at 800, 750, 700 and 650 °C, respectively. Impedance analysis indicated that the performance of cathode-supported cell was determined essentially by electrode polarization resistance, which suggested that optimizing electrodes was especially important for improving the cell performance.

1. Introduction

As energy conversion devices, solid oxide fuel cells (SOFCs) have attracted much attention because of their higher electrical conversion efficiency, environmental friendliness and fuel flexibility. One goal of current SOFCs development is to reduce fabricating cost, which is a key issue to SOFCs commercialization. Electrode-supported configuration, either anode or cathode-supported, is one approach for reducing cost.

Presently, anode-supported SOFCs have been widely studied, and Ni/YSZ cermet is the most popular anode material. It is thermally compatible with YSZ electrolyte even if processing temperature exceeds 1400 °C, which makes manufacturing process flexible [1]. Comparatively, there has been little attention paid to cathode-supported SOFCs. Though lanthanum strontium manganate (LSM)-supported SOFCs have been successfully demonstrated by Siemens Westinghouse Power Generation with tubular design [2], the fabrication process of thin YSZ membrane on cathode supports usually needs expensive and mass production-limited vapor deposition techniques (such as PVD, EVD-CVD) at necessarily low temperature to avoid the chemical reactions between conventional LSM cathode and YSZ electrolyte [3]. However, cathode-supported cells with thin anode layer may show particular advantages when cells are operated on hydrocarbon fuels with low steam/carbon ratio. This is because most of the part of the anode layer is electro-active, which would relatively protect it from depositing carbon. In addition, it reduces nickel re-oxidation, avoiding the volume contraction and expansion resulted from the accidental anode redox cycles [4].

It is well known that co-firing process may reduce operation processes, which can effectively reduce thermal stress and reduce manufacturing costs. Hence, developing co-firing process is significant to make cathode-supported SOFCs cost-effective. Co-firing LSM-supported YSZ [5–7], $La_{0.6}Sr_{0.4}Co_{0.2}Fe_{0.8}O_{3-\delta}$ (LSCF)-supported GDC [8] and $La_{0.8}Sr_{0.2}FeO_{3-\delta}$ (LSF)-supported SDC [9] have been reported recently. However, the performances were too low to be accepted for practical application at temperatures below 800 °C.

Previous work of our group demonstrated that Pr and Nd co-doped LSM showed high electro-catalysis when used as cathode material in SOFCs [10–12]. High power density of 443 mW cm^{-2} was obtained at 650 °C by using $Pr_{0.35}Nd_{0.35}Sr_{0.3}MnO_{3-\delta}$ (PNSM)/SDC cathode material [12]. In the present study, the relatively new material, PNSM, was used as cathode. Then the PNSM-based cathode-supported cell with electrolyte membrane and anode layer was fabricated through suspension coating

* Corresponding author. Tel.: +86 551 3603234; fax: +86 551 3607627.
E-mail addresses: mfliu@mail.ustc.edu.cn (M. Liu), mgym@ustc.edu.cn (G. Meng).

0378-7753/$ – see front matter © 2008 Elsevier B.V. All rights reserved.
doi:10.1016/j.jpowsour.2008.04.039

and single-step co-firing process. The cell performance of a cell prepared as described above was studied.

2. Experimental

2.1. Preparation of PNSM/SDC cathode supports

$Pr_{0.35}Nd_{0.35}Sr_{0.3}MnO_{3-\delta}$ (PNSM), $Sm_{0.2}Ce_{0.8}O_{1.95}$ (SDC) and starch powders in a weight ratio of 6:4:2 were ball-milled in ethanol for 24 h and subsequently dried. Then, the mixed powders were pressed into pellets (20 mm in diameter, 0.8 mm in thickness) under a pressure of 450 MPa, followed by sintering at 900 °C for 2 h to get cathode supports. The PNSM and SDC powders were synthesized by an auto ignition process of metal nitrate–citric acid. More details about PNSM were described in our previous study [10].

2.2. Fabricating the bi-layer of SDC–YSZ electrolyte membrane and NiO/SDC anode layer on the cathode supports

Thin electrolyte membranes, the bi-layer of SDC–YSZ, were processed by a refined particles suspension coating technique. SDC powders, synthesized via carbonate co-precipitation process [13], were employed to make a suspension. The suspension was drop-coated on the porous cathode supports surface to make SDC layers. The YSZ (TZ-8Y, EE-Tec, Inc.) layer was coated subsequently by the same process on the SDC layer after it being dried in air at room temperature. To prepare anode layers, NiO/SDC powders prepared by gel-casting process [14], were mixed with ethyl cellulose and terpineol at a weight ratio of 4:5.7:0.3 in an agate mortar and ground to form a homogeneous slurry. The slurry was then brushed directly on the dried YSZ layer. Finally, the cathode-supported green cell was co-fired at 1300 °C for 5 h to make a single cell.

2.3. Characterization of the cell performance

The single cell was sealed on an alumina tube, and then tested from 800 to 650 °C in a home-developed cell testing system with humidified hydrogen (3% H_2O) as the fuel and ambient air as the oxidant. The voltages and output currents of the cell were measured by digital multi-meters (GDM-8145). The polarization resistance of the cells was measured using a two-probe impedance spectroscopy (Chi604a, Shanghai, Chenhua) under open circuit voltage (OCV) with an amplitude of 10 mV over the frequency range from 0.01 Hz to 100 kHz. The microstructure and morphology of the cells after testing were observed using scanning electron microscopy (SEM, model KYKY 1010).

3. Results and discussion

Because of their better performance, PNSM/SDC and PNSM/YSZ composite cathodes are usually considered. It has been reported by many researchers that new phases, such as $La_2Zr_2O_7$, $SrZrO_3$ and Sr_2ZrO_4, would be formed at the interface of strontium-substituted lanthanum manganite-based perovskite (LSM) and YSZ when sintering temperature is above 1000 °C [15,16], and the formation of such impurity phases would significantly decrease cell performance. Though the PNSM showed high stability with YSZ when sintered at 1150 °C [10], the chemical stability of PNSM/YSZ at higher sintering temperature is not investigated. In the present work, the chemical compatibility of PNSM with electrolyte materials was studied by X-ray diffraction. Fig. 1a and b shows the XRD patterns of the as-prepared PNSM/SDC and PNSM/YSZ supports sintered at 1300 °C for 5 h, respectively. As shown in Fig. 1a, the XRD pattern of the PNSM/SDC support exhibits two groups of diffraction peaks. One group belonged to the PNSM and the other was cubic fluorite phase of CeO_2. There was no impurity, indicating that PNSM was very stable with SDC. However, PNSM/YSZ showed high sintering activity, which could be easily sintered to a high density. A glossy surface of the PNSM/YSZ pellets was observed. Slight peak shifts of perovskite are detected according to the XRD patterns in Fig. 1b, though no obvious impurity phases appeared. This indicated that some reactions might have occurred between the PNSM and YSZ at high temperature.

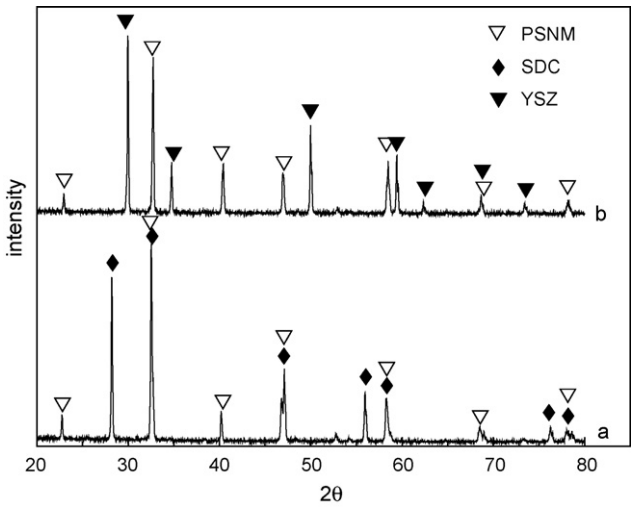

Fig. 1. XRD patterns of a: PNSM/SDC and b: PNSM/YSZ pellets sintered at 1300 °C for 5 h.

Hence, in order to avoid reacting between PNSM and YSZ, a SDC function layer was introduced between porous cathode support and YSZ electrolyte membrane. As reported by Ding [13], the nano-SDC powders prepared by a special co-precipitation had a superior sinter activity in comparison to the cathode supports, so the SDC powders were pre-calcined at 800 °C for 4 h to make it show the same shrinkage as during the co-firing process. The typical particle morphology was shown in Fig. 2, and particles exhibited a narrow size distribution. It was composed of nearly spherical particles without any hard-aggregation. The crystallite size of the powders is about 20–25 nm.

Fig. 3(a) shows the surface morphology of the as-prepared YSZ membrane. The YSZ membrane was crack-free, continuous and quite dense with uniform grains of about 0.5–1.5 μm. The result

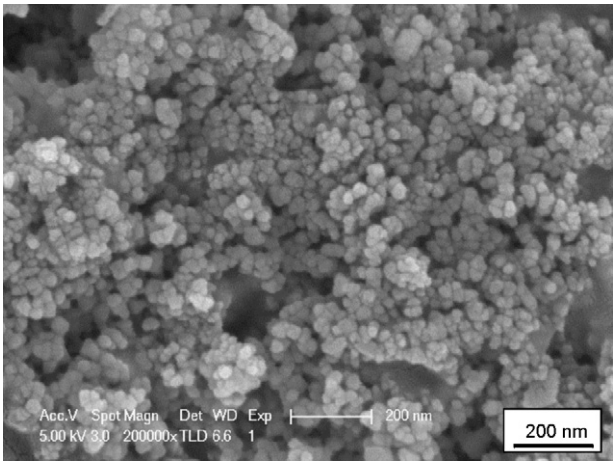

Fig. 2. TEM micrograph of SDC powders calcined at 800 °C for 4 h.

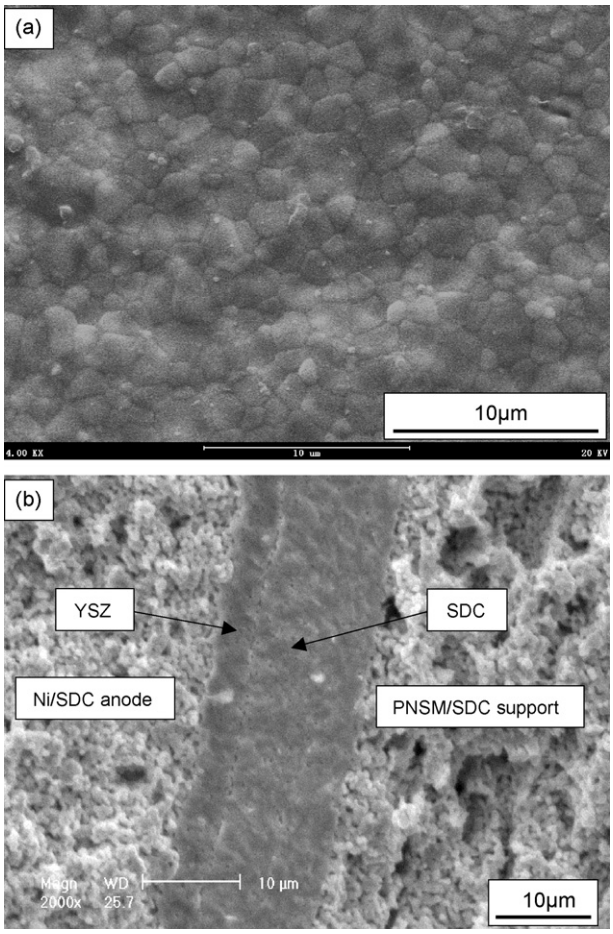

Fig. 3. (a) Surface view of the YSZ electrolyte and (b) cross-section view of the cathode-supported SOFC.

demonstrated that a dense YSZ electrolyte membrane was successfully fabricated via drop-coating and co-firing processes. Fig. 3(b) shows the cross-sectional view of the tested cell. Both SDC layer and YSZ layer were uniform, and they adhere well to the porous PNSM/SDC support and NiO/SDC anode layer, respectively. The SDC layer was about 11 μm in thickness, and the YSZ layer was about 4 μm.

Fig. 4 presents current–voltage (*I–V*) and current–power density (*I–P*) curves of as-fabricated cell using humidified hydrogen and ambient air as fuel and oxidant, respectively. The OCV values of the cathode-supported SOFC in humidified H_2 were 0.997, 1.012, 1.025 and 1.036 V at 800, 750, 700 and 650 °C, respectively. They were a little lower than the theoretical values predicted by the Nernst Equation, further indicating that the YSZ membrane was dense, as any leakage in the electrolyte membrane would lead to severely lowering of the OCV values. The lower OCV values may relate to gas leakage at the seals. As seen from the *P–I* curves, peak power densities are 657, 472, 290 and 166 mW cm^{-2} at corresponding temperatures. Though the peak power densities are much lower than that of the similarly structured anode-supported cell with Ni/YSZ–YSZ–SDC–PNSM/SDC configuration [12], the results achieved in this study was higher than that in other cathode-supported cells [5–9]. Yamahara et al. [6] and Chen et al. [5] reported that the power densities were 455 and 419 mW cm^{-2} in humidified H_2 at 800 °C for the cathode-supported cells with Co-infiltrated LSM/YSZ–$(Sc_2O_3)_{0.1}(Y_2O_3)_{0.01}(ZrO_2)_{0.89}$ (SYSZ)–SYSZ/Ni anode and YSZ/LSM–YSZ–GDC-impregnated $La_{0.75}Sr_{0.25}Cr_{0.5}Mn_{0.5}O_3$ (LSCM) anode, respectively.

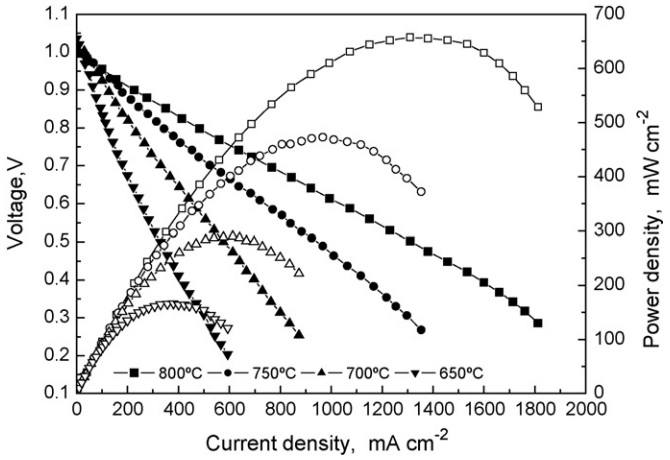

Fig. 4. Dependence of the cell voltage and power density on current density with humidified (3% H_2O) hydrogen as the fuel and ambient air as the oxidant.

To investigate the electrochemical characteristics of the cathode-supported cell, AC impedance spectra were also carried out under open-current conditions at different temperatures. As shown in Fig. 5, high-frequency real-axis interception gave ohmic resistance (R_o), and the low-frequency real-axis interception represented the total resistances (R_t) of the cell. The difference between them referred to the sum of the electrodes polarization resistance (R_p). As we know, R_o is the sum of the ohmic resistances from electrolyte, electrodes, contacts and connecting wires. The electrolyte resistance (R_e) contributed the major part as electrode materials usually are of higher conduction than electrolyte. As seen from Fig. 5, the R_o values are 0.158, 0.170, 0.194 and 0.220 Ω cm^2, respectively at 800, 750, 700 and 650 °C. The high-cell performance suggested that the SDC function layer successfully prohibited forming high resistance phases, e.g. $SrZrO_3$. However, the R_o values were slightly higher than the expected ohmic resistances calculated for 4 μm YSZ and 11 μm SDC layer with reported conductivity values [13,17]. As reported by Price et al. a SDC–YSZ solid solution would form at as low as 900 °C [18], which might significantly decrease ionic conductivity of the electrolyte [19]. The electrodes polarization resistance, including anode polarization (R_a) and cathode polarization resistance (R_c), were 0.358, 0.525, 0.961 and 1.83 Ω cm^2, respectively, at 800, 750, 700 and 650 °C, which were greatly higher than the ohmic resistance at respec-

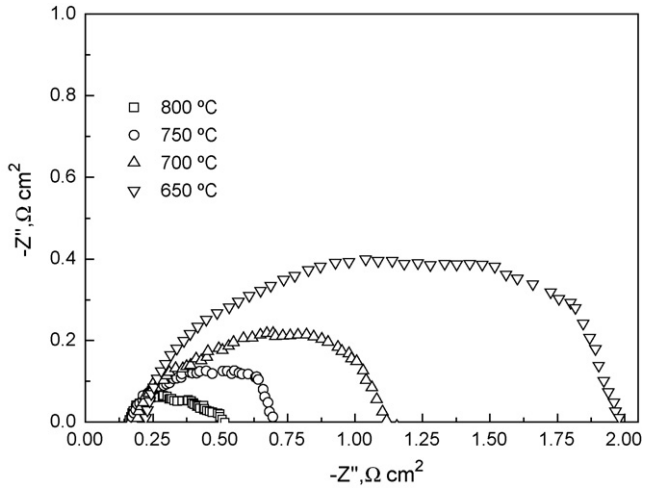

Fig. 5. Impedance spectra measured at an open circuit condition for the single cell.

tive operating temperatures. The contribution of R_p to the total cell resistance, $R_p/(R_o + R_p)$, increased as the operating temperature decreased, and achieved 90% at 650 °C. The results indicated that the cell performance was primarily governed by the polarization of electrodes, especially at lower temperatures. In our previous study, a Ni/YSZ anode-supported cell consisting of YSZ–SDC bi-layer electrolyte and PNSM/SDC cathode exhibited the R_e of 0.35 $\Omega\,cm^2$ and the R_p of 0.49 $\Omega\,cm^2$ at 650 °C [12]. Although the two cells had similar constituents and the YSZ electrolyte layer was even thinner in this work, the higher electrodes polarization resistance (1.83 $\Omega\,cm^2$) caused a lower cell performance. The difference in electrodes polarization resistance might result from the different sintering temperature of the cathode. As reported by Jørgensen et al. [20], sintering temperature significantly influenced the polarization resistance. In the present work, the PNSM/SDC was sintered at 1300 °C for 5 h to obtain dense electrolyte layer, while PNSM/SDC cathode in the anode-supported cell was only sintered at 1000 °C for 2 h [12]. The higher sintering temperature would make supports denser and grains larger. This decreased the active three phase boundaries (TPB) between electrode, electrolyte and gas phase, leading to an increase in the electrodes polarization resistance. That would be also responsible for the concentration polarization observed in Fig. 4, where negative curvature is observed at 800 °C when the current density is higher than 1.5 A cm^{-2}. Hence, in order to improve the cathode-supported cell performance at intermediate temperatures, reducing sintering temperature is an effective way, which would be studied in the future.

4. Conclusions

PNSM/SDC cathode-supported SOFC with dense SDC/YSZ electrolyte membrane and porous NiO/SDC anode layer was successfully fabricated through suspension coating and single-step co-firing processes, which are cost-effective technologies. With humidified hydrogen as fuel and ambient air as oxidant, the peak power densities of 657, 472, 290 and 166 mW cm^{-2} were obtained at 800, 750, 700 and 650 °C with open circuit voltages of 0.997, 1.012, 1.025 and 1.036 V, respectively. The cost effective processes and good cell performance suggested a potential application of cathode-supported SOFCs operating in intermediate temperatures. The study of AC impedance spectroscopy technique indicated that the electrodes polarization resistance dominated the total cell resistance, as well as cell performance.

Acknowledgements

The authors wish to acknowledge funding for this project from specialized research fund for the doctoral program of higher education (20060358034) and National Natural Science Foundation of China (50572099 and 50730002).

References

[1] L.C. De Jonghe, C.P. Jacobson, S.J. Visco, Annual Reviews of Materials Research 33 (2003) 169–182.
[2] S.C. Singhal, K. Kendall, High-temperature Solid Oxide Fuel Cells: Fundamentals, Design and Applications, Elsevier, 2003.
[3] J. Van Herle, R. Ihringer, R.V. Cavieres, L. Constantin, O. Bucheli, Journal of the European Ceramic Society 21 (2001) 1855–1859.
[4] K. Yamahara, C.P. Jacobson, S.J. Visco, X.F. Zhang, L.C. de Jonghe, Solid State Ionics 176 (2005) 275–279.
[5] X.J. Chen, Q.L. Liu, S.H. Chan, N.P. Brandon, K.A. Khor, Electrochemistry Communications 9 (2007) 767–772.
[6] K. Yamahara, C.P. Jacobson, S.J. Visco, L.C. De Jonghe, Solid State Ionics 176 (2005) 451–456.
[7] H. Orui, K. Watanabe, M. Arakawa, Journal of Power Sources 112 (2002) 90–97.
[8] Y. Liu, S. Hashimoto, H. Nishino, K. Takei, M. Mori, Journal of Power Sources 164 (2007) 56–64.
[9] B. Lin, W.P. Sun, K. Xie, Y.C. Dong, D.H. Dong, X.Q. Liu, J.F. Gao, G.Y. Meng, Journal of Alloys and Compounds (2007), doi:10.1016/j.jallcom.2007.1010.1063.
[10] M.F. Liu, D.H. Dong, L. Chen, J.F. Gao, X.Q. Liu, G.Y. Meng, Journal of Power Sources 176 (2008) 107–111.
[11] D.H. Dong, M.F. Liu, K. Xie, J.F. Gao, X.Q. Liu, G.Y. Meng, Journal of Power Sources 175 (2008) 272–275.
[12] M.F. Liu, D.H. Dong, R.R. Peng, J.F. Gao, J. Diwu, X.Q. Liu, G.Y. Meng, Journal of Power Sources 180 (2008) 215–220.
[13] D. Ding, B.B. Liu, Z.N. Zhu, S. Zhou, C.R. Xia, Solid State Ionics (2007), doi:10.1016/j.ssi.2007.1011.1015.
[14] Y.H. Yin, W. Zhu, C.R. Xia, G.Y. Meng, Journal of Power Sources 132 (2004) 36–41.
[15] M.C. Brant, L. Dessemond, Solid State Ionics 138 (2000) 1–17.
[16] K. Yang, J.H. Shen, K.Y. Yang, I.M. Hung, K.Z. Fung, M.C. Wang, Journal of Power Sources 159 (2006) 63–67.
[17] K.C. Wincewicz, J.S. Cooper, Journal of Power Sources 140 (2005) 280–296.
[18] M. Price, J.H. Dong, X.H. Gu, S.A. Speakman, E.A. Payzant, T.M. Nenoff, Journal of the American Ceramic Society 88 (2005) 1812–1818.
[19] S.Q. Hui, J. Roller, S. Yick, X. Zhang, C. Deces-Petit, Y.S. Xie, R. Maric, D. Ghosh, Journal of Power Sources 172 (2007) 493–502.
[20] M.J. Jørgensen, S. Primdahl, C. Bagger, M. Mogensen, Solid State Ionics 139 (2001) 1–11.